Steel and Composite Structures, *Vol. 17*, *No. 6* (*2014*) *851-865*
DOI: http://dx.doi.org/10.12989/scs.2014.17.6.851

Experimental study on seismic performance of partial penetration welded steel beam-column connections with different fillet radii

Hanbin Ge [*1], Liang-Jiu Jia [2a], Lan Kang [3b] and Toshimitsu Suzuki [4c]

[1] *Deptartment of Civil Engineering*, *Meijo University*,
1-501 Shiogamaguchi, *Tempaku-ku*, *Nagoya*, *468-8502*, *Japan*
[2] *Advanced Research Center for Natural Disaster Risk Reduction*, *Meijo University*,
1-501 Shiogamaguchi, *Tempaku-ku*, *Nagoya*, *468-8502*, *Japan*
[3] *School of Civil Eng. and Transportation*, *South China University of Technology*,
Wushan RD., *Tianhe District*, *Guangzhou*, *510006*, *China*
(*Former Japan Society for the Promotion of Science Research Fellow*, *Meijo Univ.*, *Japan*)
[4] *Hiroshima Machinery Works*, *Mitubishi Heavy Industries*, *Ltd.*,
5-1 Ebaokimachi, *Naka-ku*, *Hiroshima*, *730-8642*, *Japan*

(*Received June 11*, *2014*, *Revised July 24*, *2014*, *Accepted July 28*, *2014*)

Abstract. Full penetration welded steel moment-resisting frame (SMRF) structures with welded box sections are widely employed in steel bridges, where a large number of steel bridges have been in operation for over fifty years in Japan. Welding defects such as incomplete penetration at the beam-column connections of these existing SMRF steel bridge piers were observed during inspection. Previous experiments conducted by the authors' team indicate that gusset stiffeners (termed fillets in this study) at the beam-web-to-column-web joint of the beam-column connections may play an important role on the seismic performance of the connections. This paper aims to experimentally study the effect of the fillet radius on seismic performance of the connections with large welding defects. Four specimens with different sizes of fillet radii were loaded under quasi-static incremental cyclic loading, where different load-displacement relations and cracking behaviors were observed. The experimental results show that, as the size of the fillet radius increases, the seismic performance of the connections can be greatly improved.

Keywords: connection detail; welding defect; cyclic loading; beam-column connection; thick-walled steel member

1. Introduction

It is reported that there is a high risk that strong earthquakes will attack Japan in recent years, so there is an urgent need to re-evaluate seismic performance of existing steel bridges which have

*Corresponding author, Professor, E-mail: gehanbin@meijo-u.ac.jp
[a] Ph.D., E-mail: lj_jia@hotmail.com
[b] Associate Professor, Dr., Eng., E-mail: connielan@tom.com
[c] Dr., Eng., E-mail: toshimitsu_suzuki@mbe.mhi.co.jp

http://www.techno-press.org/?journal=scs&subpage=8 ISSN: 1229-9367 (Print), 1598-6233 (Online)

been in operation for over fifty years, especially for those where there are defects at the welds resulting in partial penetration welds. On the other hand, it was reported that there were un-welded parts at the corner of the beam-column connection in existing full penetration welded SMRF bridge piers due to the complicated plate assembling sequences, poor accessability, or improper welding procedure (Miki and Sasaki 2005). Moreover, welding defects such as incomplete penetration were also observed during inspection of highway steel bridge piers, where full penetration welding is required in Japan (e.g., Morikawa *et al*. 2002). The welding defects can induce severe strain concentration at the weld root of the beam-column connections in bridge piers, and it has a great potential for the connections to fail prematurely in a brittle mode after cyclic large displacement loading during a strong earthquake event. Besides, the welded connections are more susceptible to brittle fracture due to the existing crack-like defects. To date, there is still no guideline to evaluate the seismic performance of the existing steel bridges with welding defects in Japan. To prevent fracture in steel bridge piers, a simple rule based on a limit strain of $20\varepsilon_y$ (initial yield strain) obtained from pushover analysis results was suggested for the plate assemblies and members in the piers in Japan (Usami 2006, JSCE 2008). Obviously, this rule is too simple to effectively prevent fracture and improve the seismic performance, which will overestimate the seismic performance of steel piers sometimes (Ge *et al*. 2007a). Therefore, an effective approach to evaluate the seismic performance of existing welded steel piers is urgently required to avoid extensive damage as that occurred in former strong earthquakes (e.g., Bruneau *et al*. 1996) in areas with high seismic risks. Proper countermeasures to improve the seismic performance of existing steel piers are also of great importance from the viewpoint of safety for human life and property.

A number of studies on seismic performance of welded framed structures under seismic loading (e.g., MacRae and Kawashima 2001, Yamao *et al*. 2002, Ge *et al*. 2007a, b, 2013, Hsu *et al*. 2011, Linzell and Nadakuditi 2011, Ma *et al*. 2011, Bazzaz *et al*. 2012, Chen *et al*. 2012, Erfani *et al*. 2012, Luo *et al*. 2012, Soy 2012, Zahrai and Jalali 2014) were carried out. A series of experimental and analytical studies on seismic performance of cantilever piers and beam-column connections with welded box sections have been carried out in the authors' laboratory (e.g., Ge and Luo 2011, Ge and Kang 2012, Kang and Ge 2013, Jia *et al*. 2014). In previous studies, it was found that the location of crack initiation can change due to the existence of gusset stiffeners (termed fillets in this study) at the beam-web-to-column-web joint, which may improve the seismic performance of the connections.

This paper aims to study the effect of the fillet radius size on the seismic performance of the beam-column connections with a large welding defect, and enrich the experimental data of beam-column connections with welded box sections under cyclic large displacement loading. In this study, cyclic large displacement loading tests on four thick-walled beam-column connections with different fillet radii were carried out, where a welding defect of a large incomplete penetration depth was introduced into the full penetration welded connections. The experimental results indicate that the seismic performance of the connections is closely related with the size of the fillet radius. A distinguished failure process, i.e., cracking of the welds followed by local buckling of the fillets, was found for the specimen with the largest fillet radius during the test. As the fillet radius increases, both the crack initiation and propagation will be greatly delayed, which will thus result in more ductile hysteretic responses of the beam-column connections under cyclic large displacement loading.

2. Experimental program

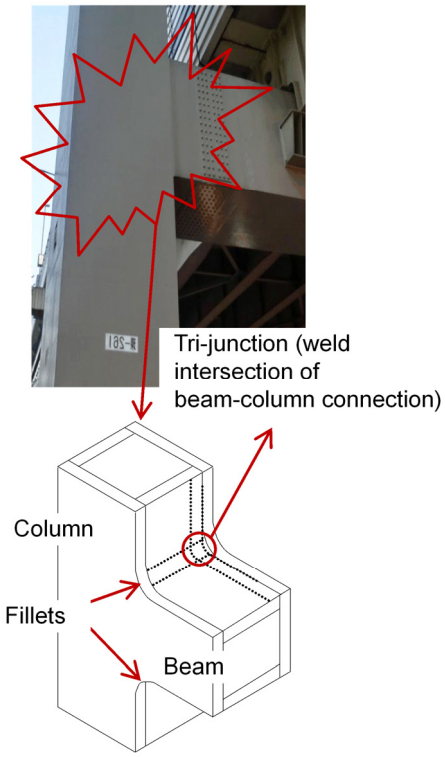

Fig. 1 Beam-column connection in steel moment-resisting frame piers

Table 1 Measured geometrical dimensions of specimens (Unit: mm)

Specimens	h	h_1	h_2	h_3	h_c	L	L_1	L_2	L_3	B	D	t	R	a	s	r_a
S30-8-5-R-VC-MD	858	168	164	16	165	769	225	225	225	175	175	12.07	5	10.0	6.8	2.8
S30-8-15-R-VC-MD	860	168	164	16	164	769	225	225	225	175	176	12.22	17	6.9	6.4	3.9
S30-8-30-R-VC-MD	860	168	164	16	163	769	225	225	225	175	176	12.22	29	7.0	9.4	5.1
S30-8-100-R-VC-MD	858	168	164	16	166	767	225	225	225	175	176	12.20	101	9.7	9.6	3.3

Notes:
(1) Notation of test specimens, e.g., S30-a-OO-R-VC-MD, S = steel; 30 = value of the width-to-thickness ratio parameter, R_f, multiplied by 100; a = incomplete penetration depth; R = R finish; VC = variable amplitude cyclic loading; MD = modified weld leg length
(2) h = column height; L = beam length; B = flange width of beam and column; D = web width of beam; h_c = web width of column; t = thickness; R = curvature radius of the fillet; s = weld leg length; r_a = size of weld throat

2.1 Configuration of specimens

Four specimens of unstiffened beam-column connections with the same incomplete penetration depth were designed to simulate the welded connections in the thick-walled SMRF bridge piers as illustrated in Fig. 1. The configuration of the specimens is illustrated in Fig. 2, where the radius of

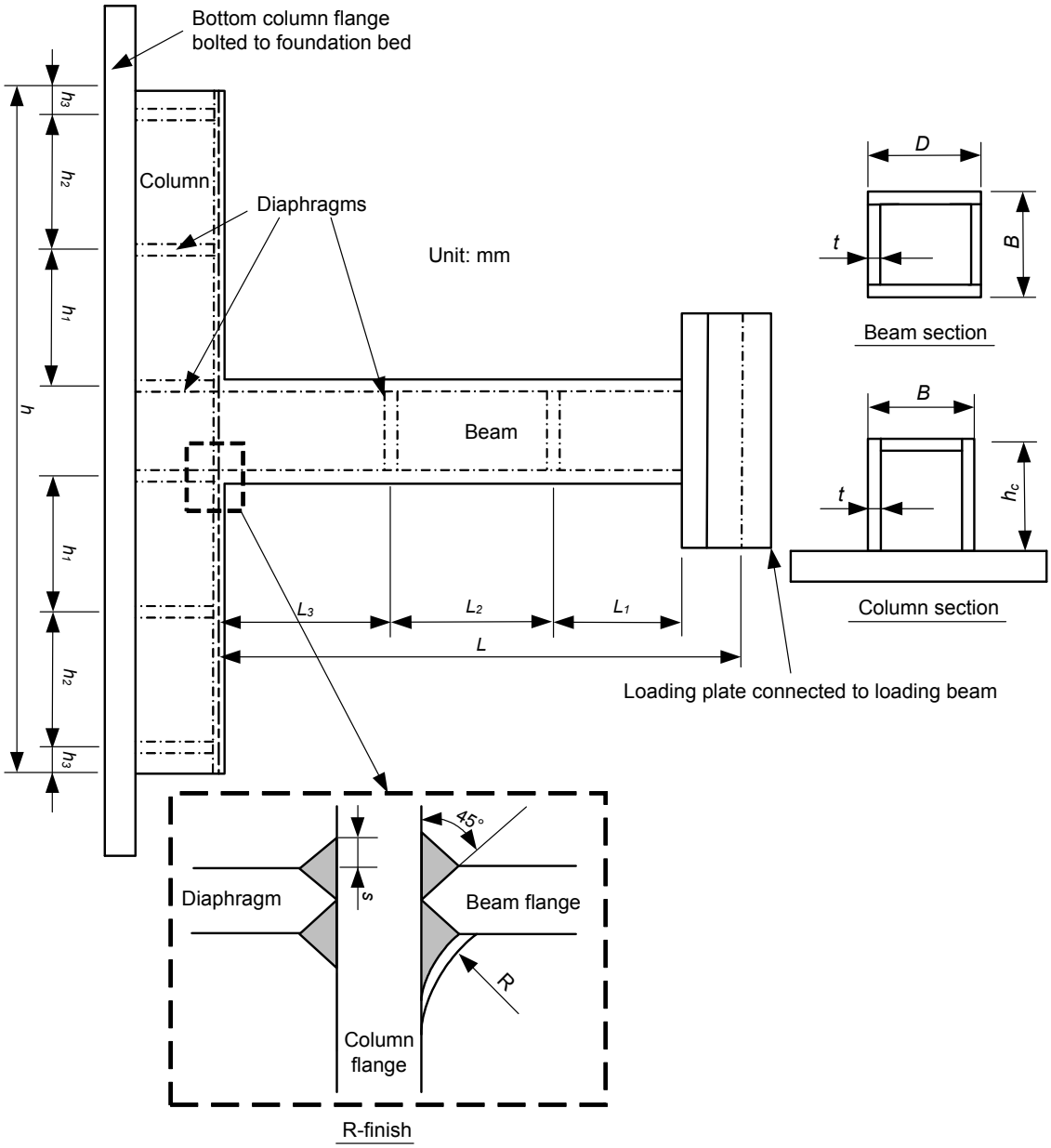

Fig. 2 Configuration of specimens

the fillet at the beam-web-to-column-web joint ranges from 5 mm to 100 mm (about 7% to 45% of the beam height). Actual dimensions of the specimens were measured before tests, which are listed in Table 1, where the numbering of the specimen, "S30-a-OO-R-VC-MD" denotes: S = steel, 30 = the value of the width-to-thickness ratio parameter, R_f, multiplied by 100, a = incomplete penetration depth, OO = fillet radius at the transition of the beam-web-to-column-web joint, R = finish type for the connections, VC = variable amplitude cyclic loading, MD = modified weld leg

Table 2 Structural parameters of the specimens

Specimens	R_f	$\bar{\lambda}$	H_y (kN)	δ_y (mm)
S30-8-5-R-VC-MD	0.254	0.376	141	5.83
S30-8-15-R-VC-MD	0.254	0.378	139	5.83
S30-8-30-R-VC-MD	0.254	0.378	139	5.83
S30-8-100-R-VC-MD	0.254	0.376	141	5.83

Note:
R_f = width-to-thickness ratio parameter; $\bar{\lambda}$ = slenderness ratio parameter; H_y = lateral yield load; δ_y = yield displacement

Table 3 Coupon test results of base metal

σ_y (MPa)	ε_y (%)	σ_u (MPa)	ε_f (%)	ν	E (GPa)	E_{st} (GPa)	ε_{st} (%)
384	0.182	532	25.7	0.285	211	4.6	2.21

Note: σ_y = yield stress, ε_y = yield strain, σ_u = tensile strength, ε_f = average strain at fracture, ν = Poisson's ratio, E = Young's modulus, E_{st} = strain hardening modulus, ε_{st} = strain at initiation of strain hardening

length from former studies carried out by the authors. The base metal of the columns and beams was made of SM490YA, which is currently widely applied to steel bridges in Japan. Both the columns and the beams were of welded rectangular sections, and the wall thickness was all designed as 12 mm considering the capacity of the loading device. The structural parameters of the specimens are listed in Table 2, and the mechanical properties of the base metal, cut along the rolling direction, are given in Table 3, where the average fracture strain, ε_f, is calculated from the measured elongation within a gage length after fracture of the coupons.

In practice, full penetration welding at the beam-column connections of the SMRF piers is commonly required, while sometimes this cannot be satisfied due to welding defects and un-welded part. To simulate the lack of complete penetration, four specimens were manufactured by partial penetration welding with the same incomplete penetration depth, a, of 8 mm in this study, which is larger than that of former specimens with the value of 5 mm. Since it has been found that a larger value of a will result in a higher potential for the connections to crack first at the weld root of the tri-junction part as illustrated in Fig. 1. The effects of the fillet radius on the seismic performance of the beam-column connections will be more specific, since the cracking mechanisms may be close to each other for all the specimens. The incomplete penetration as illustrated in Fig. 2, were introduced to the four corners at the beam-column connections. Two diaphragms were designed inside the beam members with intervals of L_1, L_2, from the right ends of the beams. Likewise, six diaphragms were also added inside the column members. The left column flange was replaced by a thick plate, to simplify the boundary conditions of the beam-column connection, since the main concern in this study is the cracking behaviors at the four corners of the beam-column connections. To simulate the actual connections where there are fillets with very small radius at the beam-flange-to-column-flange joint as illustrated in Fig. 3, the weld beads at the joint were smoothed with a small radius of 5 mm. Besides, a small radius of at least 5 mm is necessary due to difficulty in welding the tri-junction part as shown in Fig. 4. A loading plate was welded to the right end of the beam to connect with a loading beam using high strength bolts. Both the assembling and welding sequences of the plates of the beam-column connections were the

same as those employed in practice. A small width-to-thickness ratio parameter, R_f, was selected to avoid the influence of local buckling of the member plates, which may result in premature decrease in the loads and make the problem more complicated. Therefore, a width-to-thickness ratio parameter, R_f, of 0.25 defined in Eq. (1) was determined.

$$R_f = \frac{b}{t}\sqrt{\frac{12(1-\nu^2)}{\pi^2 \cdot 4n^2}}\sqrt{\frac{\sigma_y}{E}} \tag{1}$$

where b = width of beam flange, t = thickness of beam flange, σ_y = yield stress, E = Young's modulus, ν = Poisson's ratio, and n = number of sub-panels. The value of n should be 1 since the section is unstiffened.

Fig. 3 Fillets with very small radius at beam-column connections

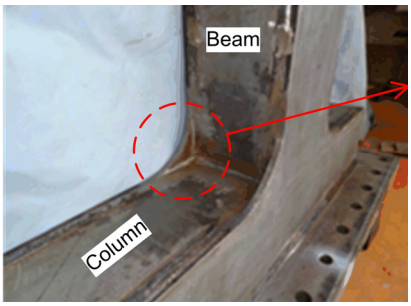

(a) Specimen S30-8-100-R-VC-MD

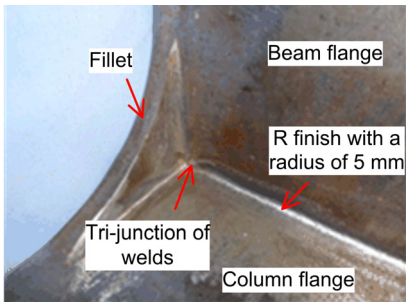

(b) Tri-junction part

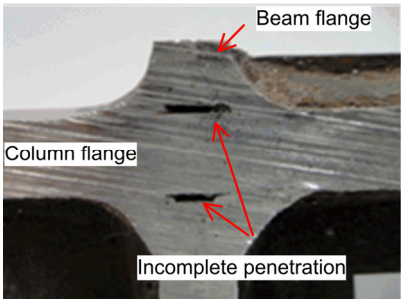

(c) Incomplete penetration

Fig. 4 Appearance of Specimen S30-8-100-R-VC-MD

The slenderness ratio parameter, $\overline{\lambda}$, of 0.38 defined according to Eq. (2) were designed to avoid premature global instability of the beams during loading.

$$\overline{\lambda} = \frac{2L}{r}\frac{1}{\pi}\sqrt{\frac{\sigma_y}{E}} \tag{2}$$

where L = beam length, and r = radius of gyration.

2.2 Test setup and loading history

The specimens were loaded using a self-balanced steel reaction frame and two horizontal actuators each with a force capacity of ± 1000 kN, and a displacement capacity of ± 500 mm, as illustrated in Fig. 5, where the beam was pin-connected to a horizontal loading frame by a loading plate bolted to the upper end of the beam to avoid local buckling of the beam, and one of the column flanges was bolted to a steel rigid foundation bed connected to the reaction frame. It should be noted that the specimen was rotated by 90 degrees to accommodate the loading system. The loading beam was pin-connected to the two actuators by a sliding beam, and the left ends of the two actuators were directly connected to a reaction column of the loading frame. Quasi-static tests were conducted under displacement control using the relative lateral displacement at the two ends of the beam of the specimen. An incremental cyclic loading history with one cycle per displacement amplitude as illustrated in Fig. 6 was employed in all the tests.

3. Experimental results

3.1 Failure modes

Before discussions on failure process of the specimens, it is necessary to give a definition for crack initiation since cracking is a main failure mode in the connections. In the current study, the

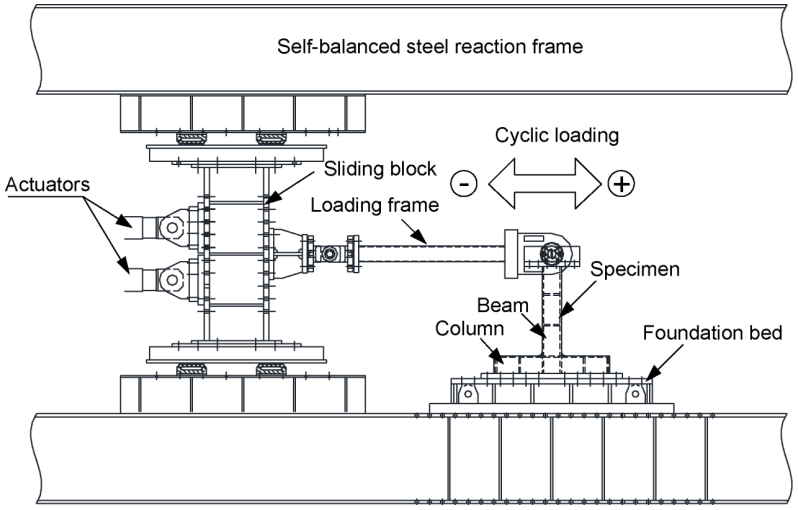

Fig. 5 Test setup

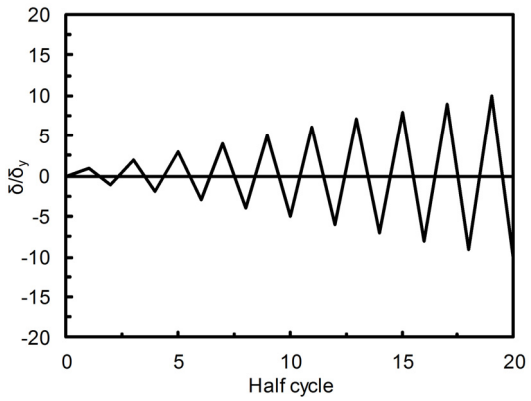

Fig. 6 Loading history

instant at crack initiation is defined when a surface crack length exceeds a value of about 1 mm which can be visualized by human eyes and a common digital camera. This definition was also adopted in previous studies by the authors (Luo *et al*. 2012, Ge and Kang 2012). This definition will overestimate the number of cycles at instant of crack initiation, since cracks initiated at the weld roots of the incomplete penetration welds, and then propagated to the surfaces of the weld beads. To compensate this limitation, numerical simulation using proper cyclic plasticity models for cyclic large plastic loading until fracture (e.g., Jia and Kuwamura 2013a) and micro-mechanism based fracture models (e.g., Jia and Kuwamura, 2013b), may give a more accurate estimation of crack initiation in future studies. Besides, the crack length is defined as the straight-line distance at two ends of a surface crack, as illustrated in Fig. 7.

Similar failure modes were observed for all the tested specimens, and the appearances of the cracked specimens after the experiments are respectively shown in Fig. 8. The experiments of the specimens were terminated when the lateral load capacities decreased to less than 90% of the

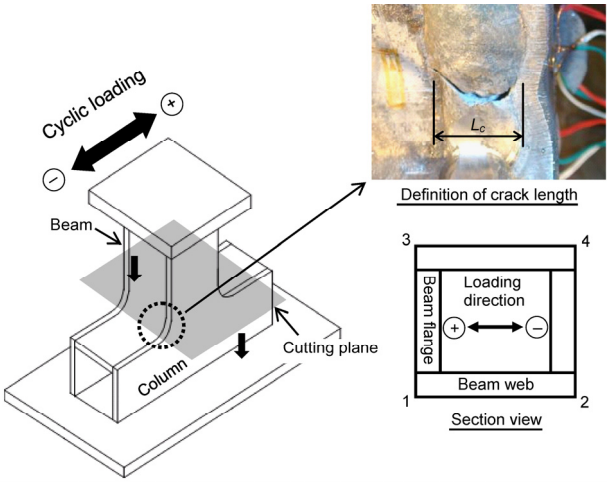

Fig. 7 Corner numbering of the connection and definition of crack length

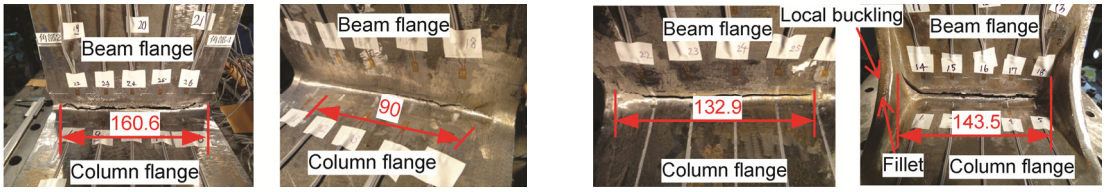

(a) S30-8-5-R-VC-MD (b) S30-8-15-R-VC-MD (c) S30-8-30-R-VC-MD (d) S30-8-100-R-VC-MD

Fig. 8 Failure modes of all the beam-column connections

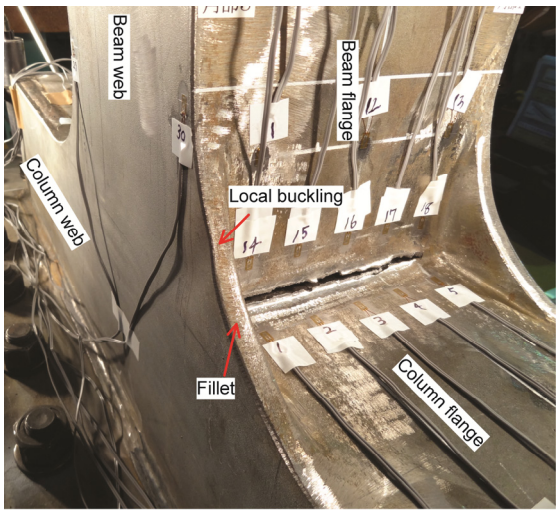

Fig. 9 Local buckling of fillet for specimen S30-8-100-R-VC-MD

Table 4 Loading histories and instants of crack initiation

Specimens	Instant at crack initiation	Height away from surface of column flange (mm)
S30-8-5-R-VC-MD	4 half cycles ($-2\delta_y \rightarrow 3\delta_y$)	2.7
S30-8-15-R-VC-MD	3 half cycles ($2\delta_y$)	2
S30-8-30-R-VC-MD	6 half cycles ($-3\delta_y$)	5
S30-8-100-R-VC-MD	8 half cycles ($-4\delta_y$)	1.7

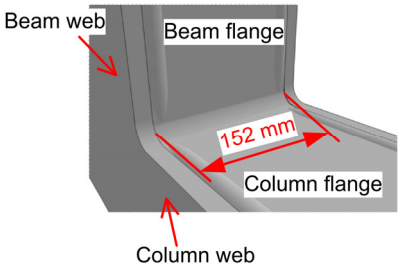

Fig. 10 Length of incomplete penetration along the beam flange width

corresponding peak loads. For all the specimens, cracks initiated from the weld roots at the beam-flange-to-column-flange joints, and propagated along the length direction of the welds at the joints. Crack first initiated and propagated along the beam-flange-to-column-flange joint for the specimen with a fillet radius of 100 mm, and then local buckling of the fillet as illustrated in Fig. 9 occurred as the displacement increased, which is distinguished from the other specimens for its large fillet size.

3.2 Comparison of crack initiation and propagation

The number of half cycles when a crack initiates, and the heights of the cracks away from the surface of column flanges, of the specimens are listed in Table 4. The locations of crack initiation are all at the weld root of the beam-flange-to-column-flange joint, while the instants at crack initiation are different. Generally, a specimen with a larger fillet radius will result in a later crack initiation. As shown in Table 1, the sizes of the weld throats are very small, and the incomplete penetration with a depth of 8 mm is similar to a pre-existing crack at the weld root of beam-flange-to-column-flange joint, which induced an early cracking initiation of the specimens in the tests. The experimental results also indicate that the specimen with a large fillet radius of 100 mm (45% of the beam height) can effectively delay the crack initiation.

Though the crack initiation locations of the specimens are similar to each other, the crack propagation behaviors are different, especially for the specimen with the largest fillet radius, S30-8-100-R-VC-MD. The crack lengths of each specimen at the end of the tests (when the load-carrying capacity decrease to less than 90% of the peak load) are shown in Fig. 8, where the crack length of Specimen S30-8-5-R-VC-MD with the smallest fillet radius of 5 mm is larger than the width of the beam flange (152 mm) as shown in Fig. 10. This indicates that the crack propagated into the beam web of the connection. However, the cracks didn't develop into the beam webs at the ends of the experiments for the other specimens with larger fillet radii. Thus, a large fillet radius can effectively delay the crack propagation into the beam web of the beam-column connection, and thus results in a more ductile connection and better seismic performance. The crack length versus number of half cycle curves given in Fig. 11, imply that cracks propagated rapidly after the crack initiation except for specimen S30-8-100-R-VC-MD, indicating a brittle failure mode at the weld of the beam-flange-to-column-flange joint for the three connections with relatively small fillet radii. The propagation speeds of the cracks tend to slow down when the cracks reach the boundaries of the beam webs. The connections were cut to observe the internal cracks as shown in Fig. 12, which indicates that all the cracks initiate from the weld roots of the incomplete penetration welds, and propagate along the weld throats at the beam-flange-to-column-flange joints. The crack propagation route is just along an angle of around 45 degrees to the vertical direction, since the sections at the weld throats are the weakest. Cracks also occurred at the internal welds at the beam-flange-to-column-flange joints as illustrated in Fig. 12(a), and propagated through the weld throats to the surfaces of internal weld beads.

3.3 Hysteretic curves

The lateral load-lateral displacement response of each test specimen is shown in Fig. 13, where the instants at crack initiation are marked with a circle in the curves. From the curves, it can be found that cracks initiated at very early stages except for the specimen with a large fillet radius of 100 mm, where the force-displacement curves are almost linear at the instants. Load-carrying capacities decreased rapidly after crack initiation in these specimens, indicating a brittle failure

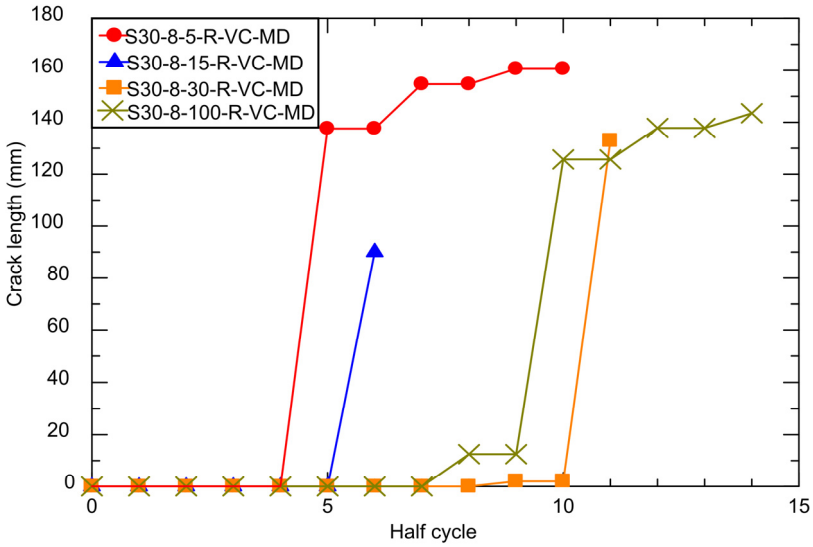

Fig. 11 Comparison of crack propagation in specimens

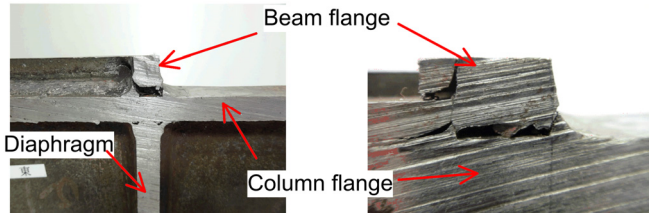

(a) S30-8-5-R-VC-MD (Corner 1) (b) S30-8-15-R-VC-ND (Corner 1)

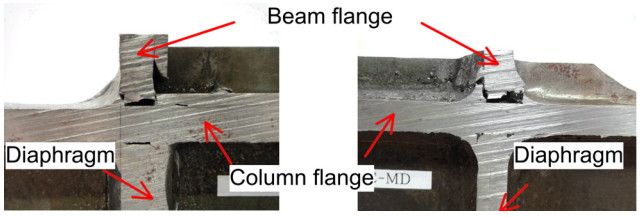

(c) S30-8-30-R-VC-MD (Corner 2) (d) S30-8-100-R-VC-MD (Corner 1)

Fig. 12 Section view of cracks in all the specimens after cutting

mode. Specimen S30-8-100-R-VC-MD exhibits a favorable stable hysteretic behavior, where the crack initiation is greatly delayed, and the crack propagation speed is also slowed down under the assistance of the large fillet at the beam-web-to-column-web joint. The different hysteretic responses are mainly due to the different crack propagation behaviors. For example, cracks propagate into the beam web soon after crack initiation for Specimen S30-8-5-R-VC-MD, which induces rapid decrease of the load-carrying capacity of the connection. However, cracks propagate within the beam flange for Specimen S30-8-100-R-VC-MD, and decrease of load-carrying

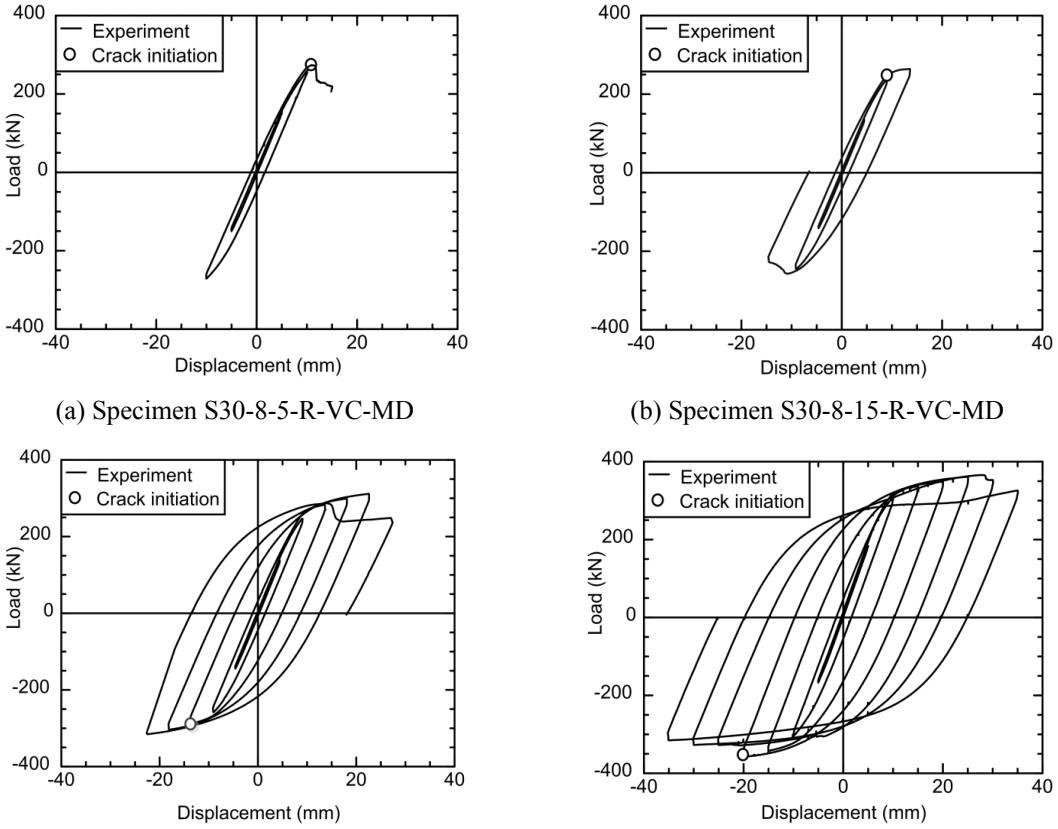

(a) Specimen S30-8-5-R-VC-MD (b) Specimen S30-8-15-R-VC-MD

(c) Specimen S30-8-30-R-VC-MD (d) Specimen S30-8-100-R-VC-MD

Fig. 13 Lateral load–lateral displacement hysteretic curves of specimens

capacity is relatively small. Besides, the peak loads at the negative side decreased after crack initiation, while the ones at positive side still increased even after crack initiation. The decrease of the load-carrying capacity at positive side for Specimen S30-8-100-R-VC-MD is due to local instability of the large fillet as illustrated in Fig. 9, but not the crack propagation into the beam webs, which is different from that of Specimen S30-8-5-R-VC-MD. Therefore, the existence of fillets with large radii at the beam-web-to-column-web joints can greatly improve the hysteretic responses of the beam-column connections in SMRF piers during a severe seismic event. This also indicates that seismic performance of existing steel bridges with large welding defects can be greatly improved through addition of large fillets.

3.4 Local strain gauge data

The strain data at the neighborhood of the connections were also measured to investigate the effect of fillet radius on strain concentration at the connections. The arrangement of the strain gauges at the beams is as shown in Fig. 14, and the data of the strain gauges near the corners of the tri-junction parts were selected and plotted in Fig. 15. The strain data at instants of crack initiation range from 0.15% to 2%, which are relative small compared with those (around 5%) of former test

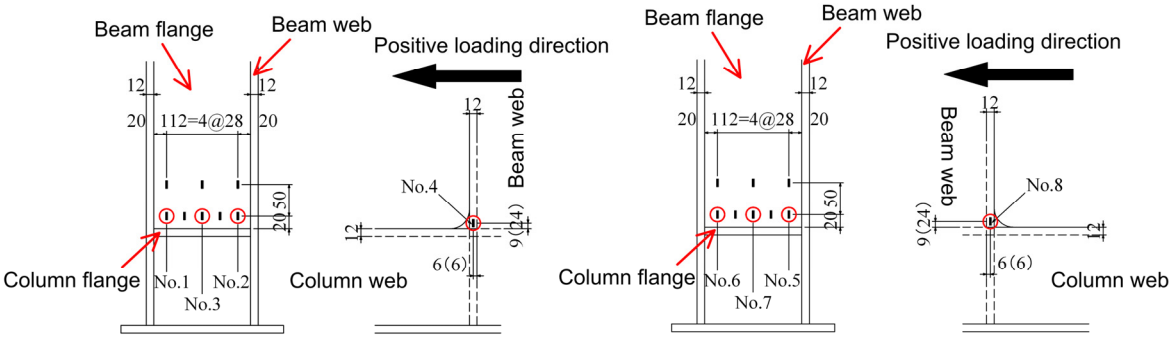

Fig. 14 Arrangement of strain gauges at connection corners

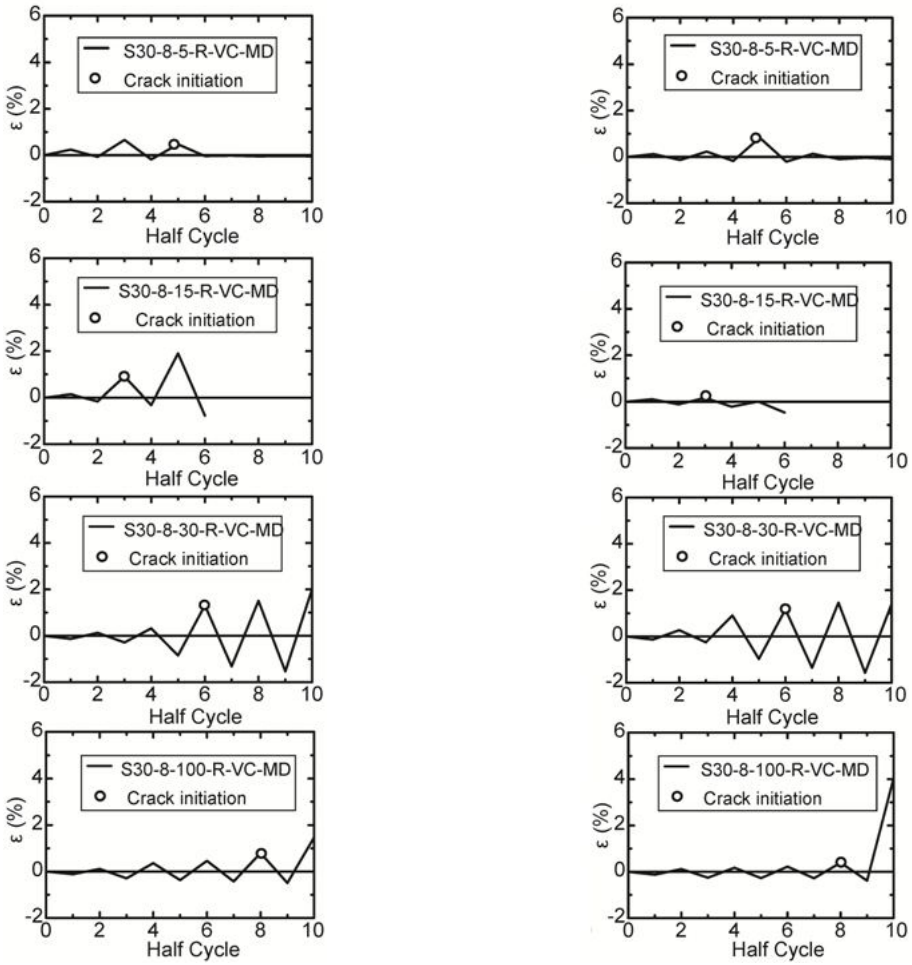

(a) Strains at Gauges 1 and 5

(b) Strains at Gauges 2 and 6

Fig. 15 Strain histories along the direction of beam length

results for specimens with an incomplete penetration depth of 5 mm and a fillet radius of 30 mm. The main reason is that the current specimens are with a larger incomplete penetration depth, and the moment resulted by the lateral load at the beam end is mainly transferred by the beam webs. It can also be found from Fig. 15 that the strains at the crack initiation of the specimen with the largest fillet radius, Specimen S30-8-100-R-VC-MD, are smaller than those of the other specimens, indicating that the existence of a large fillet radius can reduce the strain concentration at the connections.

4. Conclusions

In the present study, four steel thick-walled beam-column connections with welded box sections were tested to study the effect of gusset stiffeners (termed fillets in this study) at the beam-web-to-column-web joint on seismic performance of the connections with welding defects in steel moment-resisting frame bridge piers, where commonly full penetration welding is employed. Cyclic incremental displacement loading history was employed to simulate a strong earthquake event. Main conclusions obtained in this study are given as follows:

- Seismic performance of beam-column connections with large welding defects can be greatly improved when there are large fillets at the beam-flange-to-column-flange joints.
- Loss of load-carrying capacity of the connections with small fillet radii is due to cracking of the welds, while that of the connection with a large fillet radius is due to both cracking of the welds and local buckling of the large fillets.
- The fillet radius size doesn't affect the crack initiation location of the connections with a large incomplete penetration depth, and ductile cracks initiate at the weld roots of the beam-flange-to-column-flange joints for all the specimens in this study.
- The ductile crack initiation life isn't improved significantly for the specimens with a fillet radius ranging from 5 mm to 30 mm, but does increase greatly for the specimen with a fillet radius of 100 mm (45% of beam height).
- The crack initiation and propagation speeds for the specimen with a small radius and a large incomplete penetration depth are rapid, which exhibits brittle failure mode under cyclic large displacement loading.

Acknowledgments

The study is supported in part by grants from the JSPS Grants-in-Aid for Scientific Research (C) (No. 24560588), and the Advanced Research Center for Natural Disaster Risk Reduction, Meijo University, which supported by Ministry of Education, Culture, Sports, Science and Technology (MEXT), Japan.

References

Bazzaz, M., Kheyroddin, A., Kafi, M.A. and Andalib, Z. (2012), "Evaluation of the seismic performance of off-centre bracing system with ductile element in steel frames", *Steel Compos. Struct., Int. J.*, **12**(5), 445-464.

Bruneau, M., Wilson, J.C. and Tremblay, R. (1996), "Performance of steel bridges during the 1995 Hyogo-ken Nanbu (Kobe, Japan) earthquake", *Can. J. Civ. Eng.*, **23**(3), 678-713.

Chen, S.J., Yang, K.C., Lin, K.M. and Wang, C.C. (2012), "Experimental studies of circular composite bridge piers for seismic loading", *Steel Compos. Struct.*, **12**(3), 261-273.
Erfani, S., Naseri, A.B. and Akrami, V. (2012), "The beneficial effects of beam web opening in seismic behavior of steel moment frames", *Steel Compos. Struct., Int. J.*, **13**(1), 35-46.
Ge, H.B. and Luo, X.Q. (2011), "A seismic performance evaluation method for steel structures against local buckling and extra-low cycle fatigue", *J. Earthq. Tsunami*, **5**(1), 1-17.
Ge, H.B. and Kang, L. (2012), "A damage index-based evaluation method for predicting the ductile crack initiation in steel structures", *J. Earthq. Eng.*, **16**(5), 623-643.
Ge, H.B., Kawahito, M. and Ohashi, M. (2007a), "Experimental study on ductile crack initiation and its propagation in steel bridge piers of thick walled box sections", *J. Struct. Eng. JSCE*, **53A**, 493-502. [In Japanese)
Ge, H.B., Kawahito, M. and Ohashi, M. (2007b), "Ultimate strains of structural steels against ductile crack initiation", *J. Struct. Mech. Earthq. Eng. JSCE*, **24**(1), 13s-22s. [In Japanese]
Ge, H.B., Kang, L. and Tsumura, Y. (2013), "Extremely low-cycle fatigue tests of thick-walled steel bridge piers", *J. Bridge Eng. ASCE*, **18**(9), 858-870.
Hsu, H.L., Juang, J.L. and Chou, C.H. (2011), "Experimental evaluation on the seismic performance of steel knee braced frame structures with energy dissipation mechanism", *Steel Compos. Struct., Int. J.*, **11**(1), 77-91.
Japan Society of Civil Engineers (JSCE) (2008), *Standard Specifications for Steel and Composited Structures IV*: *Seismic Design*, Japan Society of Civil Engineers, Tokyo, Japan. [In Japanese]
Jia, L.J. and Kuwamura, H. (2013a), "Prediction of cyclic behaviors of mild steel at large plastic strain using coupon test results", *J. Struct. Eng. ASCE*, **140**(2), 04013056. DOI: 10.1061/(ASCE)ST.1943-541X.0000848
Jia, L.J. and Kuwamura, H. (2013b), "Ductile fracture simulation of structural steels under monotonic tension", *J. Struct. Eng. ASCE*, **140**(5), 04013115. DOI: 10.1061/(ASCE)ST.1943-541X.0000944
Jia, L.J., Ge, H.B. and Suzuki, T. (2014), "Effect of post weld treatment on cracking behaviors of beam-column connections in steel bridge piers", *Steel Compos. Struct., Int. J.*, 17(5), 687-704.
Kang, L. and Ge, H.B. (2013), "Predicting ductile crack initiation of steel bridge structures due to extremely low-cycle fatigue using local and non-local models", *J. Earthq. Eng.*, **17**(3), 323-349.
Linzell, D.G. and Nadakuditi, V.P. (2011), "Parameters influencing seismic response of horizontally curved, steel, I-girder bridges", *Steel Compos. Struct., Int. J.*, **11**(1), 21-38.
Luo, X.Q., Ge, H.B. and Ohashi, M. (2012), "Experimental study on ductile crack initiation in compact section steel columns", *Steel Compos. Struct., Int. J.*, **13**(4), 383-396.
Ma, H., Jiang, W. and Cho, C. (2011), "Experimental study on two types of newbeam-to-column connections", *Steel Compos. Struct.*, **11**(4), 291-305.
MacRae, G. and Kawashima, K. (2001), "Seismic behavior of hollow stiffened steel bridge columns", *J. Bridge Eng. ASCE*, **6**(2), 110-119.
Miki, C. and Sasaki, E. (2005), "Fracture in steel bridge piers due to earthquakes", *Steel Struct.*, **5**(2), 133-140.
Morikawa, H., Shimozato, T., Miki, C. and Ichikawa, A. (2002), "Study on fatigue cracking in steel bridge piers with box section and temporally repairing", *Proceedings of JSCE*, **703**(I-59), 177-183. [In Japanese]
Soy, U. (2012), "Numerical modelling of stress and deflection behaviourfor welded steel beam-column", *Steel Compos. Struct., Int. J.*, **12**(3), 249-260.
Usami, T. (2006), *Guidelines for Seismic and Damage-Control Design of Steel Bridges*, Gihodo-Shuppan, Tokyo, Japan. [In Japanese]
Yamao, T., Iwatsubo, K., Yamamuro, T., Ogushi, M. and Matsumura, S. (2002), "Seismic behavior of hollow stiffened steel bridge columns", *Thin-walled Struct.*, **40**(2), 183-197.
Zahrai, S.M. and Jalali, M. (2014), "Experimental and analytical investigations on seismic behavior of ductile steel knee braced frames", *Steel Compos. Struct., Int. J.*, **16**(1), 1-21.

BU